ISBN: 978-3-95450-262-2 ISSN: 2673-5350 doi: 10.18429/JACoW-IBIC2025-MOPMO39

DEVELOPMENT OF WALL CURRENT MONITOR ON FETS-FFA TEST RING

E. Yamakawa*, I. Gardner, K. Fazlee, Science and Technology Facilities Council, Didcot, UK

Abstract

Conceptual design studies of the FETS-FFA demonstration ring have been actively performed to confirm the reliability of a Fixed Field Alternating gradient (FFA) accelerator for a future high-power spallation neutron source, called ISIS-II. A wall Current Monitor (WCM) is a choice of non-destructive intensity monitor to evaluate the circulating proton beams from 3 MeV (about 1 MHz in revolution frequency) to 12 MeV (about 2 MHz in revolution frequency) in the FETS-FFA test ring. As the beam orbit shifts radially with beam energy in FFAs, the aperture of FETS-FFA WCM will be about 700 mm horizontally. The maximum mean circulating beam current is about 100 mA and tomographic and Schottky measurements require a bandwidth of 370 MHz (100 harmonics). This is a challenge for such a large monitor. A half-width demonstration WCM (demo-WCM) was designed and manufactured to benchmark numerical simulations and to understand monitor responses. Whilst measured frequency band was shorter than expected, 1% intensity resolution was achieved in demo-WCM. In this paper, the detail design study as well as the signal response of the demo-WCM will be presented.

INTRODUCTION

The FETS-FFA test ring is a small-scaled demonstration FFA accelerator to confirm its reliability and suitability for high-power operation in ISIS-II facility [1]. The frequency bandwidth required for a beam current monitor is from the fundamental frequency (a few MHz) up to 100 harmonics of the RF frequency at 3.74 MHz. This range is sufficient for tomographic measurements and is adequate for Schottky measurements for the FETS-FFA. To meet the requirements, a WCM has been chosen as the bunched beam intensity monitor for the FETS-FFA. The challenge in designing the FETS-FFA WCM is to achieve the physics requirements while accommodating a large horizontal aperture that covers the excursion from injection to extraction (~700 mm). The propagation patterns of the image current across the resistance will also vary with beam positions, leading to different time responses on each resistor and affecting the frequency characteristics of the monitor. To better understand the signal response from a large aperture of WCM, a half-scale demo-WCM was designed and tested at Rutherford Appleton Laboratory.

DESIGN OF DEMO-WCM

While the tentative design of vacuum chamber for the FETS-FFA features a racetrack shape with an internal aperture of 700 mm×80 mm, the chamber size of demo-WCM was constructed by 344.5 mm×50 mm to handle and test the monitor more easily, allowing for efficient evaluation of its performance characteristics. The vacuum gap was filled by alumina ceramics (ϵ=9.4) owing to its good strength and thermal stability. According to the stress analysis conducted on a similar ceramic spacer for the RF cavity, the minimum thickness of the ceramic gap was determined to be 22 mm in the FETS-FFA. This will need to be tested under vacuum in the future. The characteristic impedance of ceramic gap (Z_c) can be computed by $Z_c = 377 \cdot d/W/\sqrt{\epsilon_r}$ where d is the gap length and W is the mean circumference of the ceramic gap with the dielectric constant of ϵ_r. By adopting the gap length of 22 mm and thickness of 22 mm in the demo-WCM, the characteristic impedance of the ceramic gap is estimated to be 2.96 Ω (R_g), providing a higher cutoff frequency of about 710 MHz along with an estimated capacitance of 76.2 pF for the ceramic gap. The ceramic spacer was covered by a flexible PCB where chip resistors were attached in parallel to the beam direction. Two different cores: FT3M [2] and FR68 [3] were prepared for testing, similar to the WCM used in Fermilab [4]. These cores aim to achieve a bandwidth of several GHz by employing different cores. The interior size of the racetrack shape of the core is 414.5 mm×75 mm with thickness of 25 mm and the length of 25 mm. The monitor components were fastened to the chamber flanges using bolts and enclosed within a shield box made by 1.2 mm copper sheets. Three input ports were positioned at the centre of the monitor aperture with resistors of 1 kΩ, allowing for the measurement of monitor responses at different input positions within the aperture. Six solid wires were placed along the PCB board, both in the middle and at the edges of the aperture, to read out the output signals as shown in Fig. 1.

FREQUENCY RESPONSE

Analytical formulae of the equivalent circuit of the monitor show the expected frequency bandwidth in Table 1 with the expected capacitance ($\epsilon_0\epsilon_r S/d$) of the ceramic gap (d) of 76.2 pF, the measured resistance of 3.12 Ω across the ceramic gap and measured inductance of 17.0 µH in FT3M, 0.98 µH in FR68 and 17.1 µH in combined FT3M and FR68 respectively.

Table 1: Expected Bandwidth for Different Cores with the Inductance of Cores at 10 kHz for FT3M and at 1 MHz for FR68 Measured by the LCR Meter

Cores	Lower [kHz]	Higher [MHz]
FT3M	31 (μ_r at 10 kHz)	670
FR68	22 (μ_r at1 MHz)	670

* emi.yamakawa@stfc.ac.uk

ISBN: 978-3-95450-262-2 ISSN: 2673-5350 doi: 10.18429/JACoW-IBIC2025-MOPMO39

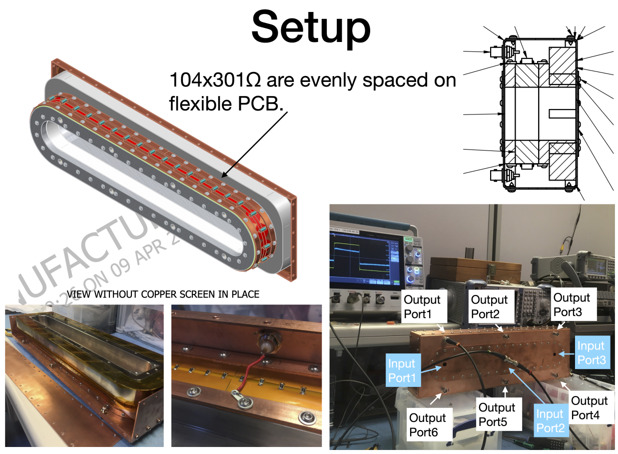

Figure 1: 2D and 3D schematics of demo-WCM on top left and right in this figure. Two pictures on the bottom left present side and top view of the monitor. The signal cable connected to the BNC output port on the outside of the box.

The frequency characteristics of the monitor were then measured by a Vector Network Analyser (VNA) by assessing the transmission coefficient (S_{21}) between the input and output ports for different cores. The input power from VNA fed in three different input ports with a resistance of 1 kΩ as shown in Fig. 2 and was shorted to the shield box. The output signals in frequency and phase were averaged across the six ports of the monitor. The high cutoff frequency is about 200 MHz for FT3M core and is lower than expected. CST simulations were conducted using High Frequency Time Domain (HFTD) solver, importing a 3D CAD drawing of the monitor with lumped elements that has a total resistance of 2.96 Ω across the ceramic gap when power was applied to input port2. The frequency characteristics between the measurements and the simulation model were similar especially in the range of about 500 kHz and 100 MHz. The combined usage of the two different cores did not extend frequency bandwidth, so the monitor equipped with FT3M core is focused on in the following studies.

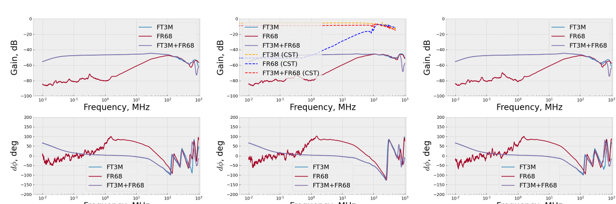

Figure 2: Frequency characteristics and its phase of the monitor with different inductive cores: FT3M, FR68 and combined of FT3M and FR68 for different input ports: port1 (left), port2 (middle) and port3 (right). For port2, the computed CST results were also shown.

TIME RESPONSE

Figure 3 shows the output signals with a pulsed input signal of 2.5 mA and 300 ns width, which is equivalent to the 1% intensity resolution required in the FETS-FFA. This signal is input to ports 1 and 2. The closer the output port was from the input port, the ringing on the rising and falling edges were enhanced. This may be caused by the microwaves in the beam direction, resonating at the resistors as shown in Fig. 4. The microwave induced by the excitation source propagates also in radial directions. To investigate how the current signals go azimuthally along the ceramic spacer, the current was input to output port4. The output signal from other output ports were monitored as shown in Fig. 5. The closer the output ports were to the input port, the shorter the time differences between the input and output signals become. Additionally, the separation of output ports from the input induced significant resonances at high frequencies. This could be caused by the complexity of signal interactions from the input.

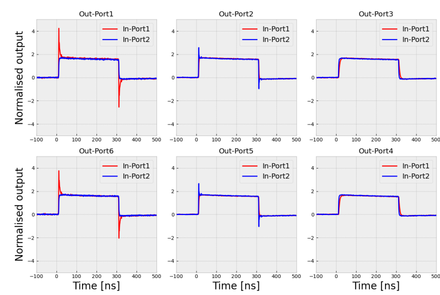

Figure 3: Output signals from each output port when feeding the signal from the input port2. The rising and falling edge of input pulsed signal was 1 ns.

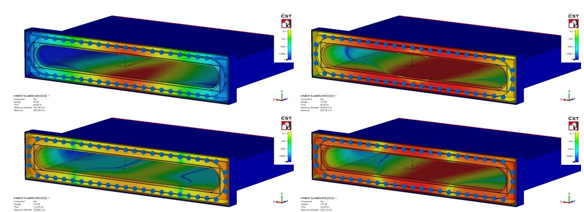

Figure 4: Microwave propagation in the full scale design of WCM in CST. In this model, the quantity of parallel resistors was 48 with individual resistor of 1.56×48 Ω.

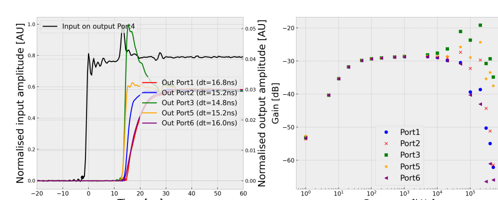

Figure 5: Frequency response (right) and rising edge (left) of output ports when the input current of 0.2 A was applied to the output port4. Time differences were computed when the signal crossed at 5 time greater than the noise level.

The position dependence of beam on the output port signals can be mitigated by averaging all output signals as shown in Fig. 6. The decay time constant (τ) of about 3 µs for different input ports were estimated by fitting a function of $e^{-t/\tau}$ with $\tau = L/R$ where L is the inductance of FT3M core and R is the resistance across the ceramic spacer. In the simulation model, the simple design of signal cables between

ISBN: 978-3-95450-262-2 ISSN: 2673-5350 doi: 10.18429/JACoW-IBIC2025-MOPMO39

one side of copper stripe and BNC connectors were included as output ports (50 Ω terminated). The HFTD solver in CST was used to run time domain simulations with 300 ns pulse width with rise and fall times of 1 ns. The average decay constant over six output ports in CST was about 5 µs that is about a factor of 1.5 longer than the reality.

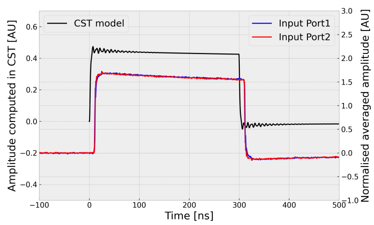

Figure 6: Averaged output signals normalised by the input amplitudes when the input current of 2.5 mA was applied on the input ports 1 and 2, compared to the expected pulse signal in CST model.

ELECTRONICS

To average the signals from all output ports and to boost the gain at low frequencies below 30 kHz (the lower cutoff frequency of the monitor), a summing amplifier was developed as shown in Fig. 7. The maximum gain of amplifier was approximately four, achieved using parallel resisters of 1.5 kΩ on each port, along with two variable resistors on the board (indicated by $R7$ and $R8$ in Fig. 7). A capacitance of 10 nF was used to extend the low frequency bandwidth. Figure 8 shows the frequency characteristics and time response of the demo-WCM with the summing amplifier. The circuit provides stable gain down to a few kHz as expected. The decay constants were improved to about 6 µs with the amplifier of HTS3001 [5], compared to 3 µs without amplifier. Further adjustment could improve this.

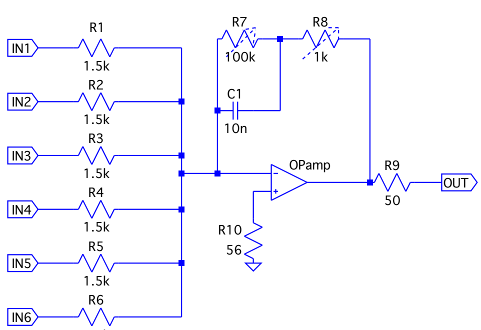

Figure 7: Schematic diagram of the test board circuit of summing amplifier. The variable resistors of 100 kΩ at $R7$ and 1 kΩ at $R8$ were used.

DIFFERENT NUMBER OF RESISTORS ACROSS THE GAP

Figure 9 plots the frequency and pulse characteristics for different quantities of resistors across the ceramic gap. A smaller number of resistors resulted in resonances at frequencies exceeding 100 MHz, which were mitigated by using a larger numbers of resistors across the spacer.

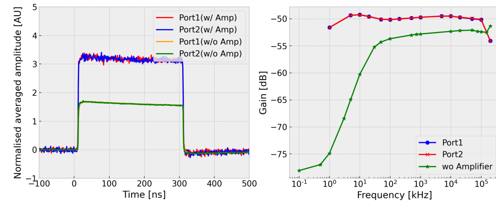

Figure 8: Right: frequency characteristics with and without summing amplifiers. Left: averaged output signals of demo-WCM with and without summing amplifier when the input current of 2.5 mA was applied on the input ports 1 and 2.

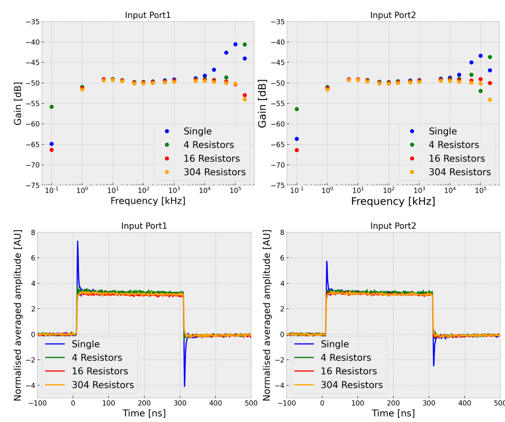

Figure 9: Frequency characteristics (top) and pulse shapes (bottom) when the input was in the ports 1 and 2 for different numbers of resistors across the ceramic gap.

CONCLUSION

A demonstration WCM has been designed and manufactured to benchmark the CST simulation model and to understand monitor responses better. The measurement of the frequency characteristics has revealed the monitor constructed with the FT3M core showed the best performance for the FETS-FFA WCM. However, the higher cutoff frequency of the monitor has been found to be lower than that of the CST model, and this is attributed to the interaction of input signals with the resistors over the ceramic gap. The resonances at high frequencies have been varied with the quantity of resistors used across the gap, finding the importance of resistor quantity in controlling resonance behaviour within the system. It has been confirmed that these resonances and the position dependencies of the beam within the chamber aperture can be mitigated by averaging signals across several output ports, facilitated by the summing amplifier with frequency adjustable circuit. Further analysis will be required to address unwanted resonances at high frequencies, with the aim of extending the frequency band to 370 MHz for the FETS-FFA test ring.

ISBN: 978-3-95450-262-2 ISSN: 2673-5350 doi: 10.18429/JACoW-IBIC2025-MOPMO39

REFERENCES

[1] J.-B. Lagrange *et al.*, "Progress on Design Studies for the ISIS II Upgrade", in *Proc. IPAC'19*, Melbourne, Australia, May 2019, pp. 2075–2078. doi:10.18429/JACoW-IPAC2019-TUPTS068

[2] Proterial Ltd., https://www.proterial.com/e/products/soft_magnetism/finemet.html

[3] Fair-Rite Products Corp., https://fair-rite.com/68-material-data-sheet/

[4] J. Crisp and B. Fellenz, "Tevatron Resistive Wall Current Monitor", *J. Instrum.*,vol. 6, p. T11001, 2011. doi:10.1088/1748-0221/6/11/T11001

[5] THS3001 420MHz, High-Speed Current-Feedback Amplifier. https://www.ti.com/product/THS3001